Journal of Magnetism and Magnetic Materials 529 (2021) 167836

Contents lists available at ScienceDirect

Journal of Magnetism and Magnetic Materials

journal homepage: www.elsevier.com/locate/jmmm

Analysis of temperature dependence in ferrofluid optical transmission dynamics after magnetic field commutation

Ángel Sanz-Felipe *, Juan Carlos Martín

Applied Physics Dept., University of Zaragoza, C/ Pedro Cerbuna, 12, 50009 Zaragoza Spain

ARTICLE INFO

Keywords:
Ferrofluid temperature dependence
Magneto-optical evolution
Temperature-dependent viscosity
Relaxation response

ABSTRACT

The influence of temperature on the ferrofluid magneto-optical response after magnetic field commutation is studied. Its contribution to the diffusion and mobility of the ferrofluid nanoparticles is considered by means of thermal agitation and the temperature-dependent viscosity of the fluid. Experimental responses after magnetic field switch on and off show a significant dependence on temperature. Taking into account both mentioned thermal influences, a qualitative description is provided, in which viscosity turns out to play an important role. In addition, a model based on an adaptation of a paramagnetic gas theory is used to analyze the transmission relaxation evolution after magnetic field switch off. The results are in good agreement with the experimental measurements, demonstrating the validity of this adaptation to consider the temperature dependence of this response.

1. Introduction

Ferrofluids, or magnetic fluids, are colloidal systems formed by magnetic nanoparticles immersed in a carrier fluid. Under exposure to an external magnetic field, the particles rotate to align their magnetic dipoles along the field lines, which also lead them to aggregate in chains parallel to the magnetic field direction due to their mutual interactions [1,2]. These phenomena induce changes in the ferrofluid optical properties, making them of great interest for potential photonic applications: variable attenuators, modulators, polarizers or optical magnetic field sensors [3–7].

Magneto-optical behavior in ferrofluids is highly dependent on many parameters to such an extent that a wide variety of responses can be obtained even with the same stimulus [2,8,9]. During the last decades, many authors have investigated the implications of some ferrofluid intrinsic parameters (particle's size, concentration and coating), and measurement conditions (magnetic field intensity and orientation, and the light beam wavelength) [2,9–12]. Some of these parameters intervene through different contributions: for instance, particle size and temperature are involved in both thermal agitation, particle mobility through the fluid and particle magnetization, which establishes their magnetic response and mutual interactions. All this makes the complete description and prediction of the ferrofluid magneto-optical response a tough but necessary task face to optimization of their promising applications.

Ferrofluid properties concerning thermal dependence offer interesting possibilities for heat transfer and magneto-thermal pumping [13–15], friction controlling [16], alternating magnetic field heating for hyperthermia [17,18], and even modifying acoustic properties [19]. Face to photonic applications, this dependence provides the opportunity for temperature sensing by means of its implementation in devices primarily based on optical fibers. A change in temperature combined with exposure to a magnetic field can modify the ferrofluid refractive index and, therefore, its optical transmission or any other optical magnitude of interest for sensing [5,20,21]. This property is useful even in absence of the external magnetic field [3]. However, the characterization of these devices is usually directly empirical or based on a slight theoretical background.

In the literature, models for ferrofluids' temperature-dependent optical properties are usually focused on the role of thermal agitation. Its effect is a trend towards random orientation of magnetic dipoles, in opposition to their orientation trend along the magnetic field direction. The quotient between magnetic and thermal energy takes part as the key factor in this kind of approaches [22], commonly replaced by the so-called coupling constant which describes the ease of particle chains formation [2,11,23,24]. Although the most fundamental dependence of the magneto-optical response on temperature has been already observed [23], this theoretical treatment has some limitations: on the

* Corresponding author.
E-mail address: angel_sf@unizar.es (Á. Sanz-Felipe).

https://doi.org/10.1016/j.jmmm.2021.167836
Received 2 December 2020; Received in revised form 19 January 2021; Accepted 4 February 2021
Available online 24 February 2021

one hand, it refers only to a static situation (typically when a stable phase is reached), so that the aggregation process and the consequent transient optical response after magnetic field commutation are obviated. Thus, the response time is not studied even though is not typically negligible and highly dependent on the sample intrinsic parameters [4,9]. Besides, viscosity dependence on temperature is not included, despite its expectable influence on the particles motion and, therefore, on the magneto-optical response, both in magnitude and speed.

The aim of this work is to delve into the temperature dependence in ferrofluids optical transmission evolution, both after magnetic field switch on and off. In order to do so, series of measurements at different temperatures have been registered and analyzed. Attention has been paid to the amount of optical transmission change induced on the ferrofluid by magnetic field application, but also to its temporal evolution both after magnetic field switch on and off. In order to explain the trends observed after magnetic field switch on, a simple qualitative reasoning involving both thermal agitation and fluid viscosity is proposed. Concerning the evolution after magnetic field switch off, an analytical model based on an adaptation of a paramagnetic gas theory is employed to quantitatively check its dependence on temperature, as well as the ability of this model to describe this response.

In Section 2, the experimental procedure and results are provided. Section 3 is devoted to qualitatively analyze the temperature-dependent results after the magnetic field switch on. In Section 4, the optical transmission relaxation after the magnetic field switch off is studied.

2. Experiment

2.1. Magneto-optical setup

The experimental setup for optical transmission measurements is shown in Fig. 1. The evolution of the ferrofluid optical transmission is registered when a homogeneous external magnetic field is switched on and off. The magnetic field is generated by means of two Helmholtz coils connected to a DC current supply, and applied parallel to the incident light direction. The ferrofluid is contained in an optical glass cuvette with dimensions 9.5 mm × 36.8 mm × 2 mm (inner light path), placed in the central point between the coils. The experimental deviation of the applied magnetic field value 1 cm far from the central point between the coils is only 0.14% (1.5×10^{-3}% theoretically), mainly due to the precision of the Hall probe used to check it. Thus, given the cuvette dimensions, the applied magnetic field can be considered homogeneous throughout the sample. A He-Ne laser beam of $\lambda = 632.8$ nm is used, which is expanded and collimated in order to illuminate the maximum ferrofluid section as possible (a circular section with diameter 9.5 mm) to minimize the effect of sample inhomogeneities. The light intensity transmitted through the sample in the incident direction is detected and registered.

The ferrofluid employed is supplied by NanoMyP and contains MagP® nanoparticles suspended in water/SDS as carrier fluid. Their magnetic cores ($R_n = 50$ nm in average) are formed by magnetite. Their saturation magnetization is 26.4 emu/g, as observed in the $M-H$ curve shown in Fig. 2, measured by VSM technique. This curve has been obtained by previously eliminating the carrier fluid and any non-magnetic component from the particles. Their superparamagnetic character is also verified in the inset of Fig. 2: the total magnetization turns to zero once the external magnetic field is removed. On the other hand, a large polymeric coating (58 wt% MMA and 42 wt% EGDMA), together with the SDS surfactant, surrounds the magnetic cores, as observed via TEM images [10]. As a consequence, the complete particle has a hydrodynamic radius $R_h = 92$ nm (polydispersity index PdI = 0.176 according to the manufacturer), which ensures that the particles remain dispersed in the absence of an external magnetic field. A long term stability of the dispersion has been clearly observed: no changes in optical transmission are detected during more than an hour. The coating dimension also explains the sample slow response evolution and a complete reversibility to the initial dispersed particle distribution after exposure to the external magnetic field, as will be seen later.

The cuvette with the ferrofluid is previously brought to the study temperature. In order to do so, it is introduced in a thermal bath long enough to ensure that the entire sample reaches a homogeneous temperature. Then, it is placed in its location at the magneto-optical setup. Due to the complexity of our entire setup and its components, the initial ferrofluid temperature cannot be maintained during the measurement. For that reason, it is expected that the sample may cool towards room temperature by thermal conduction with the surrounding air. This temperature variation will be taken into account when analyzing the results. As a consequence, observation time must be selected appropriately in order to balance a long enough evolution of the magneto-optical response is observed with a sufficiently low temperature variation from the sample starting value, face to also analyze the temperature dependence in the relaxation process. Given the small size of the cuvette, any possible convective process should not be significant, but even in such a case, the temperature obtained in our results will refer to a mean value of the entire sample thanks to the beam width employed.

2.2. Experimental results

Three measurements with different initial ferrofluid temperatures have been carried out. One of them corresponds to room temperature,

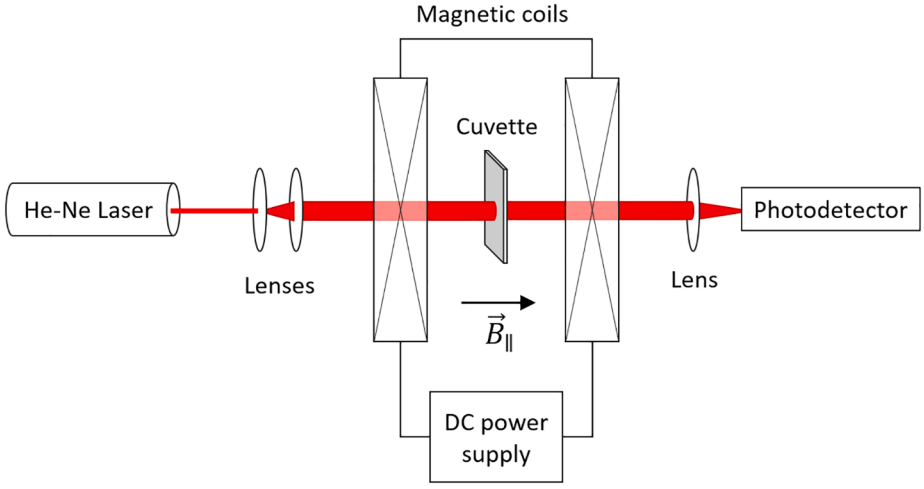

Fig. 1. Experimental magneto-optical transmission setup.

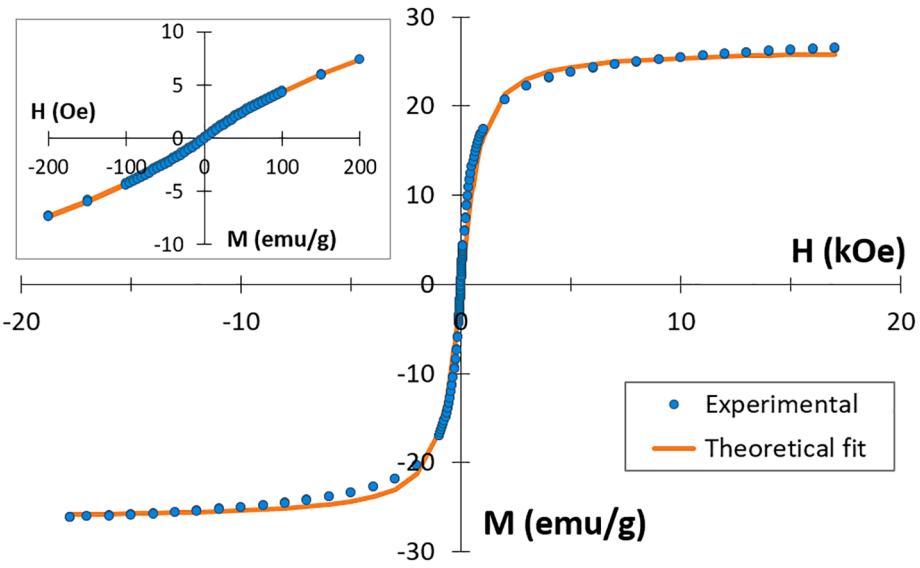

Fig. 2. $M-H$ curve of the nanoparticles' magnetic core. The response to the low magnetic field range is shown in the inset, where the monodomain character of the magnetic particles is confirmed.

22 °C, which is the typical condition used throughout the literature at studying other temperature independent ferrofluid properties. The other two are 32 °C and 60 °C. The first one has been selected in order to consider a small temperature difference but sufficient to detect a noticeable result and attributable to this single modification. The second one has been selected as a sufficiently remote range to check out the different temperature dependences that will be explained in Section 3. At $t = 0$, the power supply is switched on and a magnetic field of 72 G is generated parallel to the light beam. This magnetic field intensity has been selected as high enough to observe a considerable magneto-optical response of the ferrofluid, but also to discriminate the thermal contribution: a higher value may increase the magnetic interactions between the particles, making the temperature dependence less identifiable or even negligible. Magnetic field is applied for 180 s and then is switched off. Relaxation transmission evolution is also registered for 90 s. Nanoparticles concentration used is 7.1 mg/mL (particle mass per suspension volume), selected for being the one that maximizes the transmission changes of this ferrofluid [9].

Fig. 3 shows the transmission temporal evolution results. The optical transmission measured at each instant, T, is presented normalized to its value in absence of magnetic field, T_0: $T_n = T/T_0$. All the cases exhibit a decrease in optical transmission when the ferrofluid is exposed to the external magnetic field. The sharply decrease is related to the initial rotation of the particles and the formation of the first short chainlike aggregates as a consequence of the dipole–dipole attraction (as well as the orientation or stylizing of possible already existing aggregates). This behavior is consistent with other experimental results obtained with this sample [9,10] and other ferrofluids [25], and explained by means of an increase in the ferrofluid's light extinction due to this particle's restructuring, as justified by different theoretical [10,25,26] and numerical [9] models. As seen in Fig. 3, the decrease in transmission slows down after the initial response as the repulsive and dispersive interactions, caused or favored by the large amount of coating, make it more difficult to gather new further away particles. When the individual chains are long enough, they can coalesce laterally, inducing a reversal in the ferrofluid optical transmission trend [9,27]. This trend has been observed in this sample with longer exposures to magnetic field, although the coalescence degree is very low: no chains have been observed even with an image resolution of 2.75 μm/px [9]. Analyzing the temperature influence on this coalescence process would require improving the setup to keep the ferrofluid temperature constant. For both reasons, studying this structural stage has been discarded in this work: it would not be possible to unequivocally attribute the results to either coalescence or the constant drop in the sample's temperature. Finally, once the magnetic field is switched off, the sample transmission recovers the initial value, showing up the sample's reversibility due to the stabilizing agents mentioned above.

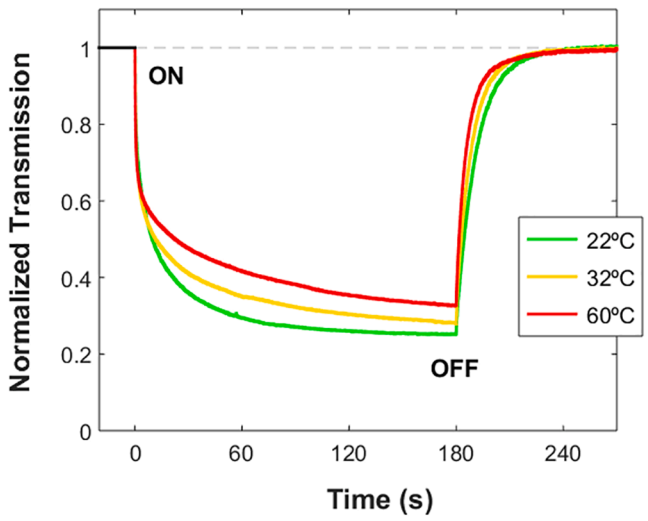

Fig. 3. Time evolution of the ferrofluid optical transmission after magnetic field switch on and off with different initial ferrofluid temperatures. The magnetic field ($B = 72$ G) is applied parallel with respect to the light beam.

A clear temperature dependence is observed in Fig. 3: the higher the temperature, the lower the optical transmission change reached. It can also be appreciated that the evolution rate depends on the ferrofluid temperature, both during the magnetic field application and after its switch off. These behaviors are explored and justified in the following section.

3. Optical transmission evolution after switch on

Results from Section 2 are employed to analyze the temperature dependence of the ferrofluid magneto-optical response. Firstly, a qualitative analysis is carried out in order to examine the different contributions of temperature to the ferrofluid intrinsic properties after the magnetic field is switched on, and therefore, to its magneto-optical

outcome.

The normalized transmission reached at the end of the magnetic field application in Fig. 3 clearly depends on the ferrofluid temperature. Not surprisingly, the lower the temperature, the higher the transmission change, as observed in [23]: in the long term, a low temperature reduces the thermal dispersive effects and, as a consequence, favors better defined magnetic dipole orientation and greater chain formation. However, for a better comparison between dynamics with different temperature, it seems convenient to renormalize the vertical axis. For this purpose, Fig. 4 shows the evolution of the transmission change relative to the maximum change reached at $t = 180$ s. This way, the change achieved at $t = 180$ s corresponds to 100% in every temperature curve. However, only the first 50 s period of magnetic field application is shown, for the sake of clarity.

Two stages in the optical transmission evolution appear:

- Stage 1: the optical transmission changes during the first 2–3 s of the ferrofluid response are favored by a higher temperature. The higher the temperature, the faster the magneto-optical response evolution.
- Stage 2: the previous trend gets reversed after few seconds and the transmission changes are then favored by a lower ferrofluid temperature. As a consequence, the final transmission changes are determined by this second dependence so that the higher the temperature, the slower the ferrofluid response.

In order to understand these behaviors, it is necessary to delve into the temperature contribution to the particle dynamics. Particle diffusion in a fluid is usually described by means of the Brownian diffusion coefficient. The higher this coefficient, the greater the effect on the particles to remain dispersed. Different coefficients are required for translational and rotational diffusion treatment, although both factors present a similar dependence on temperature [28]:

$$D_i(T) = K_i \frac{T}{\eta(T)} \tag{1}$$

where K_i, being $i = t, r$, represents a constant that depends on the particle radius in a different way for translational and rotational cases respectively: $K_t = k_B/6\pi R$ and $K_r = k_B/8\pi R^3$, being k_B the Boltzmann constant. This expression shows that the particle diffusion depends directly on the temperature, but also indirectly through the fluid viscosity, $\eta(T)$, which is usually obviated in the literature, especially in optical transmission studies [2,11,23,24]. Fig. 5 presents the viscosity of water as a function of temperature using the Vogel equation [29]:

$$\eta(T) = exp\left(A + \frac{B}{C+T}\right) \tag{2}$$

where A, B and C are constants. It should be noted that our particles are immersed in water/SDS. However, any contribution of the SDS surfactant to the fluid viscosity is difficult to estimate in our sample. For this reason, the ferrofluid viscosity has been considered that of water, whose temperature dependence is well-known. Any deviation from this value will be included in an effective diffusion coefficient in Section 4. Fig. 5 also shows the quotient $T/\eta(T)$ present in Eq. (1), which makes clear that the higher the temperature, the easier the particle dispersion in the fluid.

On the other hand, viscosity also contributes to the particles mobility: it determines the drag force suffered by the particles due to their translational and rotational movements through the fluid. Consider a small spherical particle moving at low velocities. Drag force opposing the translational motion can be considered proportional to its velocity, according to the well-known Stokes' law:

$$\vec{F}_{drag} = -C_D \vec{v} = -6\pi R\eta \vec{v} \tag{3}$$

where the drag coefficient C_D is proportional to the fluid viscosity and the particle radius [28]. Thus, taking into account Fig. 5, the higher the temperature, the lower the fluid viscosity and, therefore, the lower the drag force. The same treatment can be considered for rotational movements caused by the magnetic alignment, properly substituting the drag coefficient ($C_D = 20\pi R\eta$ [28]), so that the dependence on the fluid viscosity is analogous. In summary, the higher the temperature, the faster the particle movement but the stronger the dispersive effects, so that two simultaneous, opposite trends take place: the first one speeds up particle alignment and aggregation, the second one slows it down.

Taking into account both contributions, the two stages pointed out in Fig. 4 can be associated to both temperature effects observed in Fig. 5:

- Stage 1 is determined by the fluid viscosity dependence. Once the magnetic dipoles get aligned due to the external magnetic field application, dipole-dipole forces cause the particles to start moving to aggregate. The nearby particles are highly attracted and their initial displacements are fast and much greater than the dispersive effects. Thus, the ferrofluid evolution is mainly related to the drag force: the higher the temperature, the lower the drag force and the faster the evolution.

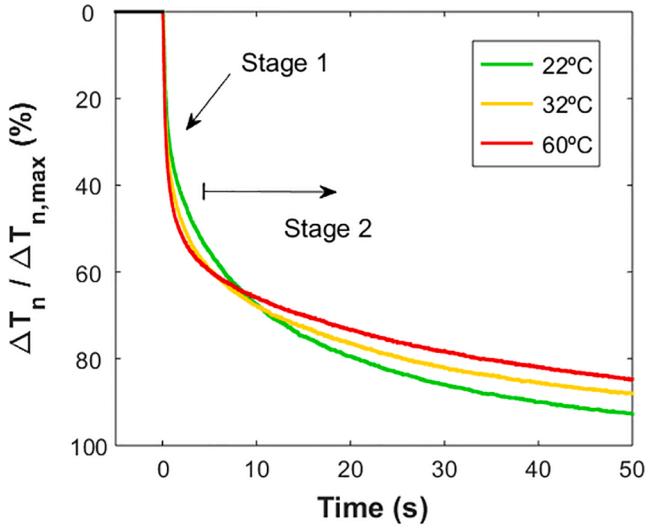

Fig. 4. Time evolution of the ferrofluid transmission change after the magnetic field switch on from Fig. 3 curves. Results are shown normalized to the maximum change reached at the end of the magnetic field application ($t = 180$ s) with each ferrofluid temperature.

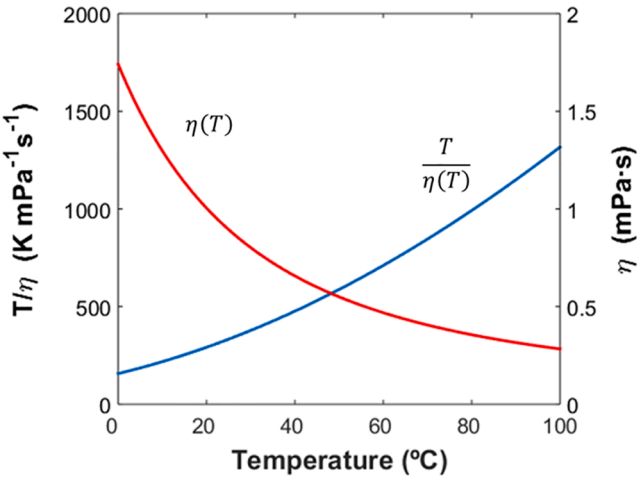

Fig. 5. Comparison between the trends of water viscosity and the quotient $T/\eta(T)$ of Eq. (1) as a function of temperature. Water viscosity has been calculated with Eq. (2) using $A = -3.72$, $B = 578.92$ K, $C = -137.55$ K [29].

- Stage 2 is determined by the thermal agitation. As the aggregation process evolves, attracting new particles is increasingly difficult: the longer the mutual distances, the weaker the mutual attraction, so that the particles displacements begin to be comparable to those of Brownian diffusion. As a consequence, growth of the induced structures slows down and so does optical transmission evolution. This contribution is the one which remains during the following evolution of the ferrofluid. Thus, the higher the temperature, the less transmission changes reached.

This way, the different transmission trends observed in Fig. 4 depending on the temperature as the ferrofluid evolves under magnetic field application are described, at least qualitatively.

4. Optical transmission relaxation after switch off

Once the magnetic field is switched off, the cause of the chain formation disappears and particles tend to redisperse throughout the fluid due to thermal diffusion. Fig. 6 shows the renormalized results from Fig. 3 during the first 50 s after the magnetic field switch off. It is clearly observed that the higher the temperature, the faster the transmission evolution, as expected from Eq. (1) since the diffusion coefficient increases with temperature (Fig. 5).

4.1. Theoretical analysis: modified Elmore's model

In order to check if the experimental results depending on the ferrofluid temperature are also quantitatively consistent, the modified Elmore's model [26] is employed. This model departs from the Elmore's expansion of a paramagnetic gas theory applied to optical transmission changes in ferrofluids [22]. Some modifications are proposed in [26] to adapt the model to a non-strictly paramagnetic gas such as a ferrofluid. The magnetic field dependence (intensity and orientation) is checked there, but since temperature is also incorporated to the model, it seems logical to apply it to our experimental results.

The normalized optical transmission of a ferrofluid exposed to an external magnetic field B can be calculated from the Elmore's model as [26]:

$$T_n = T_0^{\frac{q(a)}{q(0)}-1} \tag{4}$$

where $a = mB/k_BT$ is the ratio between magnetic energy and thermal agitation, and function q describes the cross section of the average particles' aggregate relative to that which it exhibits when it is perfectly lined up parallel to the cuvette axis. When the magnetic field is applied parallel to the light beam as in our case, function q can be obtained as [26]:

$$q(a) = 1 + q_1\frac{2L(a)}{a} + q_2\frac{8}{a^2}\left(1 - \frac{3L(a)}{a}\right) \tag{5}$$

where $L(a) = \coth(a) - 1/a$ is the Langevin function, and q_1 and q_2 are two constants characteristic of each sample. The value $q(0)$ in Eq. (4) can be deduced by substituting $a = 0$ in the latter equation. In order to consider the ferrofluid as a non-ideal paramagnetic gas, the modified Elmore's model takes into account the energy quotient a as a fitting parameter. More specific details of this assumption and the previous expressions can be found in [26].

On the other hand, when the external magnetic field is turned off, the temporal relaxation in transmission is also considered by the model through the function q in Eq. (4). The temporal relaxation is implemented by means of the rotational diffusion coefficient D_r [22]:

$$q(a,t) = c_0 + c_2L_2(a)e^{-6D_rt} + c_4L_4(a)e^{-20D_rt} \tag{6}$$

where c_0, c_2 and c_4 are constants related to q_1 and q_2, and $L_2(a)$ and $L_4(a)$ are functions related to the Langevin function, as indicated in [26]. In this expression, $t = 0$ corresponds to the instant when the magnetic field is turned off. After the mentioned modifications to the model [26], the diffusion coefficient in Eq. (6) becomes an effective diffusion coefficient, D. This way, it includes all dispersive effects in the ferrofluid: rotational and translational Brownian motion, as well as the repulsive effect of the stabilizing agents incorporated into the carrier fluid or coating the particles, which prevent them from irreversibly aggregating. In addition, any variation on the theoretical particles drag coefficient due to the micellar structure surrounding the particle, the possible particle polydispersity contribution, or other contributions to the effective ferrofluid viscosity, would also be directly included in this diffusion coefficient.

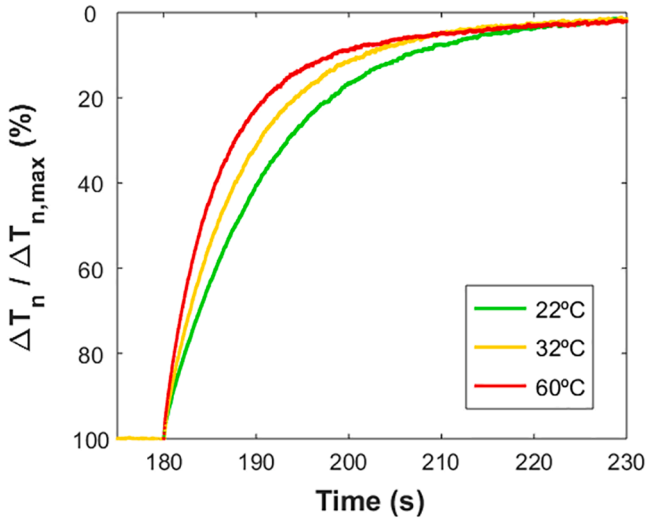

Fig. 6. Time evolution of the ferrofluid transmission change after the magnetic field switch off from Fig. 3 curves. Results are shown normalized to the maximum change reached at the end of the magnetic field application (t = 180 s) with each ferrofluid temperature.

4.2. Analysis of the results

As exposed in [26], relaxation curves obtained with the modified Elmore's model fit considerably well the experimental results when the magnetic field has been applied parallel to the incident laser beam. For that reason, it seems convenient to use this theoretical approach to analyze our experimental results. A complete series of measurements of the same ferrofluid used here at room temperature is analyzed in [26], and the rest setup and sample conditions are identical to the employed in this work. The values of q_1 and q_2 will be taken from there: $q_1 = -1.675$, $q_2 = 1.222$ ($T_0 = 0.8$ with $\varphi = 7.1$ mg/mL).

The relaxation evolution of each temperature curve in Fig. 3 after magnetic field switch off is fit to Eqs. (4) and (6). The fitting parameter D obtained for each temperature is presented in Table 1. Then, the theoretical ferrofluid temperature of each measurement can be estimated from the effective diffusion coefficients, by comparison with the value obtained in [26] for this sample at room temperature, $D(T_R)$, considering Eq. (1) as follows:

Table 1
Diffusion coefficient D obtained by fitting the relaxation response after magnetic field switch off of Fig. 3 results to the modified Elmore's model, Eq. (6). The estimated temperature for each measurement is shown in comparison to the experimental starting temperatures.

T_{exp} (°C)	T_{exp} (K)	D (rad^2/s)	T (K)
22	295	0.0158	298.5
32	305	0.0196	307.4
60	333	0.0245	317.6

$$T = \frac{D(T)\eta(T)}{D(T_R)\eta(T_R)}T_R \quad (7)$$

where T_R = 295 K and $D(T_R)$ = 0.0149 rad^2/s [26]. In Eq. (7), the theoretical temperature value must be solved by numerical methods due to its complex contribution to the fluid viscosity (Eq. (2)). The estimated temperatures from measurements in Fig. 3 are shown in Table 1.

The temperatures estimated by means of the modified Elmore's model are in good agreement with the experimental values. The deviation of the expected temperatures can be associated to the simplicity and limitations of the model to obtain quantitatively accurate results. Regarding the highest temperature, the estimated value is significantly lower than the experimental one. It should be reminded that T_{exp} corresponds to the starting temperature: the sample may have cooled towards room temperature after the first 180 s of measurement, so this result is consistent. This effect is only appreciated in this case since the difference with respect to room temperature is clearly the greatest one. Therefore, the results verify the ability of using the modified Elmore's model for considering the magneto-optical relaxation response as a function of the ferrofluid temperature.

5. Conclusions

The contribution of thermal agitation and the temperature-dependent viscosity of the ferrofluid have been considered to analyze its magneto-optical evolution after magnetic field commutation. Different responses have been detected in magnitude but also in time evolution as a function of the ferrofluid temperature, which represents an important novelty compared to previous works. Taking into account the particles' mobility and diffusion throughout the fluid has allowed explaining the different optical transmission dynamics, both after magnetic field switch on and off. As the results show, the fluid viscosity dependence on temperature plays an important role on the ferrofluid magneto-optical response that must be considered, especially for its time response.

The modified Elmore's model has allowed describing the different relaxation responses as a function of the ferrofluid temperature. The estimated ferrofluid temperatures are in agreement with the measurements carried out, showing up the ability of this model to consider the temperature dependence. On the contrary, the simplicity and limitations of this model do not allow studying the evolution during the magnetic field application since the particles aggregation process cannot be considered by such simple theoretical approach. Nevertheless, this response has been qualitatively explained by the particles diffusion and mobility as a function of temperature.

CRediT authorship contribution statement

Ángel Sanz-Felipe: Validation, Formal analysis, Investigation, Data curation, Writing - original draft, Visualization. **Juan Carlos Martín:** Conceptualization, Methodology, Resources, Supervision.

Declaration of Competing Interest

The authors declare that they have no known competing financial interests or personal relationships that could have appeared to influence the work reported in this paper.

Acknowledgements

This work was supported by the Diputación General de Aragón, project E44_17R.

References

[1] S. Odenbach, Colloidal Magnetic Fluids: Basics, Development and Applications of Ferrofluids, Springer, Berlin, 2009.
[2] M. Ivey, J. Liu, Y. Zhu, S. Cutillas, Magnetic-field-induced structural transitions in a ferrofluid emulsion, Phys. Rev. E 63 (2000), 011403, https://doi.org/10.1103/PhysRevE.63.011403.
[3] M.M. Bilal, W. Bi, F. Jaleel, Y. Luwen, M.N. Sohail, M. Irshad, J. Wa, H.A. Madni, Magnetic fluid-based photonic crystal fiber for temperature sensing, Opt. Eng. 58 (2019) 1, https://doi.org/10.1117/1.OE.58.7.072008.
[4] S. Pu, X. Chen, Z. Di, Y. Xia, Relaxation property of the magnetic-fluid-based fiber-optic evanescent field modulator, J. Appl. Phys. 101 (2007), 053532, https://doi.org/10.1063/1.2709526.
[5] L. Luo, S. Pu, S. Dong, J. Tang, Fiber-optic magnetic field sensor using magnetic fluid as the cladding, Sens. Actuators A Phys. 236 (2015) 67–72, https://doi.org/10.1016/j.sna.2015.10.034.
[6] E. Rodriguez-Schwendtner, M.-C. Navarrete, N. Diaz-Herrera, A. Gonzalez-Cano, O. Esteban, Advanced plasmonic fiber-optic sensor for high sensitivity measurement of magnetic field, IEEE Sens. J. 19 (17) (2019) 7355–7364, https://doi.org/10.1109/JSEN.736110.1109/JSEN.2019.2916157.
[7] C. Vales-Pinzón, J.J. Alvarado-Gil, R. Medina-Esquivel, P. Martínez-Torres, Polarized light transmission in ferrofluids loaded with carbon nanotubes in the presence of a uniform magnetic field, J. Magn. Magn. Mater. 369 (2014) 114–121, https://doi.org/10.1016/j.jmmm.2014.06.025.
[8] L. Chen, J. Li, X. Qiu, Y. Lin, X. Liu, H. Miao, J. Fu, Magneto-optical effect in a system of colloidal particle having anisotropic dielectric property, Opt. Commun. 316 (2014) 146–151, https://doi.org/10.1016/j.optcom.2013.11.058.
[9] Á. Sanz-Felipe, I. Barba, J.C. Martín, Optical transmission of ferrofluids exposed to a magnetic field: analysis by electromagnetic wave propagation numerical methods, J. Mol. Liq. 315 (2020), 113713, https://doi.org/10.1016/j.molliq.2020.113713.
[10] Á. Sanz-Felipe, J.C. Martín, Analysis of the optical transmission of a ferrofluid by an electromagnetic mixture law, J. Phys. D. Appl. Phys. 51 (2018), 135001, https://doi.org/10.1088/1361-6463/aab05f.
[11] S. Brojabasi, T. Muthukumaran, J.M. Laskar, J. Philip, The effect of suspended Fe_3O_4 nanoparticle size on magneto-optical properties of ferrofluids, Opt. Commun. 336 (2015) 278–285, https://doi.org/10.1016/j.optcom.2014.09.065.
[12] K.T. Wu, Y.D. Yao, H.K. Huang, Comparison of dynamic and optical properties of Fe3O4 ferrofluid emulsion in water and oleic acid under magnetic field, J. Magn. Magn. Mater. 209 (1-3) (2000) 246–248, https://doi.org/10.1016/S0304-8853(99)00704-0.
[13] M. Petit, Y. Avenas, A. Kedous-Lebouc, W. Cherief, E. Rullière, Experimental study of a static system based on a magneto-thermal coupling in ferrofluids, Int. J. Refrig. 37 (2014) 201–208, https://doi.org/10.1016/j.ijrefrig.2013.09.011.
[14] H. Yamaguchi, T. Bessho, Long distance heat transport device using temperature sensitive magnetic fluid, J. Magn. Magn. Mater. 499 (2020), 166248, https://doi.org/10.1016/j.jmmm.2019.166248.
[15] A. Jafari, T. Tynjälä, S.M. Mousavi, P. Sarkomaa, Simulation of heat transfer in a ferrofluid using computational fluid dynamics technique, Int. J. Heat Fluid Flow 29 (4) (2008) 1197–1202, https://doi.org/10.1016/j.ijheatfluidflow.2008.01.007.
[16] H.K. Moghadam, S.S. Baghbani, H. Babazadeh, Study of thermal performance of a ferrofluid with multivariable dependence viscosity within a wavy duct with external magnetic force, J. Therm. Anal. Calorim. (2020), https://doi.org/10.1007/s10973-020-09324-4.
[17] R.E. Rosensweig, Heating magnetic fluid with alternating magnetic field, J. Magn. Magn. Mater. 252 (2002) 370–374, https://doi.org/10.1016/S0304-8853(02)00706-0.
[18] S. Geng, H. Yang, X. Ren, Y. Liu, S. He, J. Zhou, N. Su, Y. Li, C. Xu, X. Zhang, Z. Cheng, Anisotropic magnetite nanorods for enhanced magnetic hyperthermia, Chem. Asian J. (2016), https://doi.org/10.1002/asia.201601042.
[19] K. Parekh, J. Patel, R.V. Upadhyay, Temperature dependent acoustic properties of temperature sensitive magnetic fluid subjected to magnetic field, J. Mol. Liq. 248 (2017) 569–576, https://doi.org/10.1016/j.molliq.2017.10.090.
[20] Y. Zhao, Y. Zhang, R. Lv, Q.i. Wang, Novel optical devices based on the tunable refractive index of magnetic fluid and their characteristics, J. Magn. Magn. Mater. 323 (23) (2011) 2987–2996, https://doi.org/10.1016/j.jmmm.2011.06.025.
[21] D. Zhang, Z. Di, Y. Zou, X. Chen, Temperature sensor using ferrofluid thin film, Microfluid. Nanofluidics 7 (2009) 141–144, https://doi.org/10.1007/s10404-008-0371-8. 10.1007/s10404-008-0371-8.
[22] W.C. Elmore, Theory of the optical and magnetic properties of ferromagnetic suspensions, Phys. Rev. 60 (8) (1941) 593–596, https://doi.org/10.1103/PhysRev.60.593.
[23] S. Brojabasi, V. Mahendran, B.B. Lahiri, J. Philip, Temperature dependent light transmission in ferrofluids, Opt. Commun. 342 (2015) 224–229, https://doi.org/10.1016/j.optcom.2014.12.073.
[24] Z. Wang, C. Holm, H.W. Müller, Molecular dynamics study on the equilibrium magnetization properties and structure of ferrofluids, Phys. Rev. E 66 (2002), 021405, https://doi.org/10.1103/PhysRevE.66.021405.
[25] J.M. Laskar, J. Philip, B. Raj, Experimental investigation of magnetic-field-induced aggregation kinetics in nonaqueous ferrofluids, Phys. Rev. E 82 (2010), 021402, https://doi.org/10.1103/PhysRevE.82.021402.
[26] F.Á. Sanz, J.C. Martin, Application of a paramagnetic gas theory to describe the magneto-optical response in ferrofluids, J. Phys. D Appl. Phys. (2020), https://doi.org/10.1088/1361-6463/abb489.

[27] D.K. Mohapatra, J.M. Laskar, J. Philip, Temporal evolution of equilibrium and non-equilibrium magnetic field driven microstructures in a magnetic fluid, J. Mol. Liq. 304 (2020), 112737, https://doi.org/10.1016/j.molliq.2020.112737.

[28] R.H. Fowler, Statistical Mechanics: The Theory of the Properties of Matter in Equilibrium, second ed., Cambridge University Press, Cambridge, 1936.

[29] Dortmund Data Bank – DDB, Liquid Dynamic Viscosity, http://ddbonline.ddbst.com/VogelCalculation/VogelCalculationCGI.exe.